INTERNATIONAL JOURNAL FOR NUMERICAL METHODS IN FLUIDS, VOL. 23, 1197–1210 (1996)

FINITE ELEMENT SIMULATION OF GUST LOADING

J. SHI*

Department of Aeronautical Engineering, Queen's University of Belfast, Belfast BT9 5AG, U.K.

AND

D. HITCHINGS

Department of Aeronautics, Imperial College, London SW7 2AZ, U.K.

SUMMARY

In the structural design of civil aircraft the critical loads are often those encountered in a gust or atmospheric turbulence. The traditional 'indicial' solution is restricted to a simple plate. In this paper a finite element formulation is proposed for an aerofoil or arbitrary shape entering a uniform sharp-edged or sinusoidal gust. The thin rotational gust front and wake in an irrotational flow field are successfully modelled by a novel superposition technique. The finite element solutions are compared with the Kussner function and results by other numerical methods. The agreement is good.

KEY WORDS: finite element method; gust

1. INTRODUCTION

Although the problem of a sinusoidally oscillating aerofoil has dominated unsteady aerodynamics because of its important application in flutter analysis, there are occasions in structural design of aircraft where the critical loads come from gust encounters. This is especially true for a civil aircraft, which only undergoes gentle manoeuvre in flight compared with its military counterpart.[1]

A simple model of atmospheric turbulence is a uniform vertical velocity profile travelling downstream at a speed $U_\infty + U_g$ (see Figure 1). The vertical velocities of the fluid particles on the left and right of the gust front have a difference equal to the gust intensity W_g, which makes the gust front a vortex sheet of uniform strength. The part of the aerofoil already in the gust changes its effective incidence. As a result, the circulation around the aerofoil needs to be adjusted to satisfy the Kutta condition, which leads to the shedding of vortices into the wake according to Kelvin's law. This process continues until the gust front approaches infinity and a steady state is thus reached.

The stationary gust, which is a gust travelling at the same speed as the mean flow, was traditionally studied by the 'indicial' method as for the problem of aerofoil motion. Kussner[2] first solved the problem of an aerofoil entering a uniform sharp-edged stationary gust, which was also addressed later by Von Karman and Sears[3] in a more general context. Their solution methods were similar to that of Theodorsen.[4] Once a response for the uniform sharp gust is obtained, the response for a gust of arbitrary shape can be determined by a convolution integral.

* Current address: Mechanical Engineering Centre, European Gas Turbines, Cambridge Road, Leicester LE8 6LH, U.K.

CCC 0271–2091/96/111197–14

Received August 1994
Revised October 1995

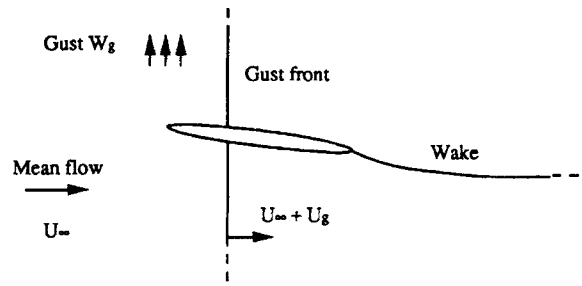

Figure 1. Uniform sharp-edged gust

An approximate numerical method for the stationary uniform sharp-edged gust has been developed by Giesing[5] and Basu and Hancock.[6] While Giesing assumed that the gust front remains straight and travels downstream at the freestream speed, Basu and Hancock represented the gust front with a uniform vorticity distribution and allowed it to be deformed.

Although in practice the gust travelling speed U_g relative to the wind speed is small and hence negligible, problems such as (i) an aeroplane or missile dropped from another plane, (ii) and aeroplane crossing the wake of or flying past another plane and (iii) a helicopter blade transversing the wake produced by itself or other blades of the rotor all imply a travelling gust.[7] In order to calculate the gust loading and aerofoil response, one needs to be able to analyse the travelling gust. In this paper both the stationary and the travelling gust will be studied. One interesting comparison between a travelling gust and an impulsively started aerofoil is that when U_g is infinite, the former equals the latter. Miles[8] first solved such a problem for a two-dimensional incompressible flow. The extension to wings in compressible and supersonic flows was carried out by Drischler and Diederich[7] through a different approach.

Another kind of gust that needs to be considered in aircraft design is the sinusoidal gust. When finding the structural response to atmospheric turbulence, one needs to know both the forces due to harmonic aerofoil motion and the forces due to a sinusoidal gust.[9] While the former has been addressed by Shi and Hitchings,[10] the latter is considered in the second part of this paper.

The sinusoidal gust model comes from the power spectral density method, which represents a random atmospheric turbulence in the frequency domain. The component of the series is a sinusoidal gust field of a particular frequency. For a reliable analysis the number of frequencies has to be large,[11] typically of the order of 100.

For the sinusoidal gust model (Figure 2) a vertical velocity field is superposed on a mean flow field. The intensity of the gust varies only in the mean flow direction. It remains constant in the perpendicular direction. The gust may travel at a different speed from U_∞, but this can be treated as a

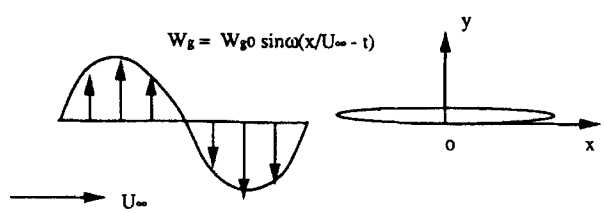

Figure 2. Sinusoidal gust

gust of modified frequency.[12] As a result, only the stationary sinusoidal gust is discussed in this paper.

Von Karman and Sears[3] and Sears[13] first solved the problem analytically for a plate. A sinusoidal gust problem for an elliptical wing in an incompressible flow was tackled by Jones.[14] Subsonic and supersonic rectangular wings were addressed by Drischler.[9] Garrick[15] found the relation between a uniform gust and a sinusoidal gust through Fourier transformation. An approximate method developed by Basu and Hancock[12] was also used to solve a thick aerofoil immersed in a sinusoidal gust field. A modification to Sear's function was made by Giesing *et al.*,[11] who established the feasibility of using a lifting surface technique for the analysis of one- or two-dimensional gust fields.

Since a finite element application to the analysis of a uniform sharped-edged gust is lacking, a finite element formulation will be given in the next two sections for both the sharp-edged (stationary and travelling) and sinusoidal gusts. The formulation is based on the success of the finite element treatment of a thin vortex sheet in an irrotational flow field described in References 10, 16 and 17. The numerical results are presented in Section 4.

2. FINITE ELEMENT FORMULATION FOR UNIFORM SHARP-EDGED GUST

The sharp-edged gust problem (Figure 3) can be posed as

$$\begin{aligned} \nabla^2\phi &= 0 && \text{in } \Omega, \\ \partial\phi/\partial n &= u_\infty && \text{on } \partial\Omega_1, \\ \Delta\phi &= f_1(s,t) && \text{on } \partial\Omega_2, \\ \partial\phi/\partial n &= 0 && \text{on } \partial\Omega_3, \\ \partial\phi/\partial n &= W_g \text{ or } 0 && \text{on } \partial\Omega_4, \\ \Delta\phi &= f_2(s,t) && \text{on } \partial\Omega_5, \end{aligned} \tag{1}$$

in which ϕ is the velocity potential and f_1 and f_2 are known functions. Only the part of $\partial\Omega_4$ on the left of the gust front has $\partial\phi/\partial t = W_g$, while on the right $\partial\phi/\partial t = 0$, where t and n denote tangential and normal directions on the boundary respectively. An obvious boundary condition on the gust front is a vertical velocity discontinuity W_g. Such a condition cannot be readily incorporated into a finite element formulation, so it is replaced by the velocity potential difference condition as in previous papers[10,16,17] for the wake.

To simplify the problem, the same assumptions as in References 10, 16 and 17 have been made for the wake, i.e. it remains straight and the wake front propagates downstream at the mean velocity. Regarding the gust front, it remains undeformed and travels at a constant speed $U_\infty + U_g$. The solution techniques for the gust problem are similar to those for the aerofoil indicial motions,[16] since

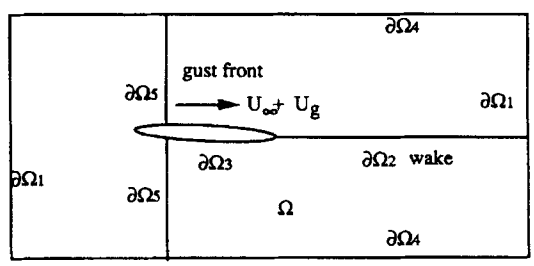

Figure 3. Definition of uniform sharp-edged gust problem

they are both transient problems involving a growing wake from the vortex shedding. The major differences are the presence of a rotational sharp-edged gust front and the time-dependent boundary condition on the outer horizontal boundaries. Thus a large part of the formulation in this section can be a direct copy of that in Reference 16 and only the modelling of the gust front is emphasized. Since the gust front has been idealized as two vertical semi-infinite thin vortex lines separated by the aerofoil and the wake, it can also be simulated by velocity potential differences.

The total solution is decomposed into five subsolutions,

$$\phi = (\phi_1 + \phi_5 + \phi_4 + \phi_3 + \Delta\Gamma_t\phi_2), \tag{2}$$

where $\nabla^2\phi_i = 0$ in Ω and $\partial\phi_i/\partial n = 0$ on $\partial\Omega_3$ $(i = 1, \ldots, 5)$, since the aerofoil is stationary. However, on the other boundaries we have

	$\partial\phi/\partial n$ on $\partial\Omega_1$	$\Delta\phi$ on $\partial\Omega_2$	$\partial\phi/\partial n$ on $\partial\Omega_4$	$\Delta\phi$ on $\partial\Omega_5$
ϕ_1	1	0	0	0
ϕ_2	0	f_1	0	0
ϕ_3	0	f_2	0	0
ϕ_4	0	0	0	f_3
ϕ_5	0	0	W_g or 0	0

where f_1, f_2 and f_3 are known and will be discussed next. On $\partial\Omega_4$ only the part inside the gust has $\partial\phi/\partial n = W_g$, otherwise $\partial\phi/\partial n = 0$, where n is the normal of the boundary.

The first time-independent part ϕ_1 corresponds to the mean incidence effect and is equal to ϕ_0 in Reference 17. The modelling of the wake and vortex shedding is exactly the same as in Reference 16, e.g. here ϕ_2 and ϕ_3 are the equivalent of ϕ_2 and ϕ_1 in Reference 16; f_1 and f_2 are thus defined accordingly. As a consequence, we will not repeat the detailed formulation.

Here ϕ_4 is defined by the moving gust front. From Figure 4 we can derive the velocity potential difference between a pair of points on the left and right sides of the gust front by integrating the velocity $W_g + V(y)$ on the left of the gust from ϕ_R to the aerofoil ϕ_a and then integrating the velocity $V(y)$ on the right of the gust from the aerofoil ϕ_a to ϕ_R. Because we only have a gust velocity W_g on the left of the gust, f_3 in equation (2) is

$$f_3 = \phi_L - \phi_R = (\phi_L - \phi_a) + (\phi_a - \phi_R) = \int_0^S [W_g + V(y)]dy - \int_0^S V(y)dy = W_g S. \tag{3}$$

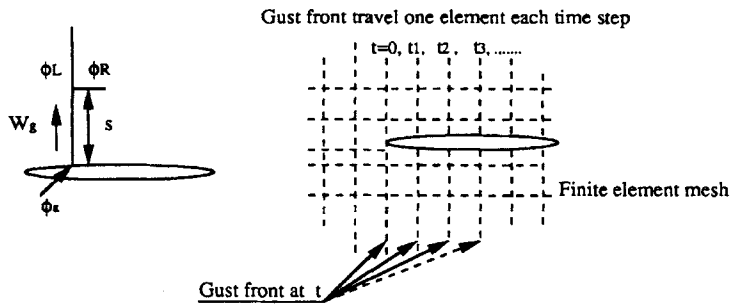

Figure 4. Gust front modelling

Similarly, f_3 for the lower half of the gust front can be found. As a result, we can replace the nodal velocity potential on one side of the gust front by the sum of their difference and the velocity potential on the other side. The consequent modification to the element matrix is exactly the same as for an element on the wake.[10,16,17]

The last component ϕ_5 represents the upwash produced by the moving gust. Only the part of $\partial\Omega_4$ already reached by the gust front has a non-zero upwash. The three separate time-dependent solution components ϕ_3, ϕ_4 and ϕ_5 are retained merely for the purpose of clear illustration. They can in fact be combined into one quantity in the computer implementation to improve the solution efficiency. At the same time we want to emphasize that ϕ_1 and ϕ_2 are solved once only, since they do not vary with time. Moreover, the coefficient matrix is factored once only too.

At the beginning of the time integration, $t=0$, the gust front is at the leading edge. The circulation around the aerofoil is zero and the length of the wake is also zero. The flow is made up of the mean flow ϕ_1 and the gust terms ϕ_4 and ϕ_5. At the end of the first time step a vortex is added to the flow. These vortices later form the wake. Within each time step $[t_{n-1}, t_n]$ the gust front (ϕ_4) is made to travel one element length l_e, while the wake (ϕ_3) at t_{n-1} moves a distance $\Delta s = l_e U_\infty/(U_\infty + U_g)$ with a newly shed vortex ϕ_2 added to the wake. The vortex shedding is modelled slightly differently from that in Reference 16, where the wake front moves one element length in each time step, because now the time step size is controlled by the advance of the gust front. When the gust front reaches the downstream mesh boundary, it can either be neglected or remain there, because the mesh boundary is so far from the aerofoil that the influence of the gust front is trivial or a steady state has been reached.

The circulation increment $\Delta\Gamma_t$ ($\Gamma_t = \Gamma_{t-1} + \Delta\Gamma_t$) in (2) is determined from the classical Kutta condition[16]

$$V_5^{\mathrm{TE}} + V_4^{\mathrm{TE}} + V_3^{\mathrm{TE}} + \Delta\Gamma_t V_2^{\mathrm{TE}} = 0 \quad \text{or} \quad \Delta\Gamma_t = -(V_5^{\mathrm{TE}} + V_4^{\mathrm{TE}} + V_3^{\mathrm{TE}})/V_2^{\mathrm{TE}}, \tag{4}$$

where the superscript TE denotes the trailing edge of the aerofoil. Other forms of trailing edge conditions are possible, eg. one can enforce zero pressure difference or make the tangential velocity difference equal to the vorticity.[10] In the transient analysis[5] it was found that the results are not particularly sensitive to the special trailing edge condition used. Moreover, in this paper we are mainly concerned with aerofoils of sharp trailing edge, hence we simply adopt the form of equation (4).

As in Reference 16, the velocities can be found by differentiating ϕ in equation (2) with respect to x and y as

$$U = U_1 + U_5 + U_4 + U_3 + \Delta\Gamma_t U_2, \qquad V = V_1 + V_5 + V_4 + V_3 + \Delta\Gamma_t V_2 \tag{5}$$

and the pressure is

$$\begin{aligned} P(t_n) = &-(\rho/2)(U_1^n U_1^n + V_1^n V_1^n) - \rho[U_1^n(U_5^n + U_4^n + U_3^n + \Delta\Gamma_n U_2^n) - \rho V_1^n(V_5^n + V_4^n + V_3^n + \Delta\Gamma_n V_2^n)] \\ &-(\rho/\Delta t_n)[(\phi_5^n + \phi_4^n + \phi_3^n + \Delta\Gamma_n \phi_2^n) - (\phi_5^{n-1} + \phi_4^{n-1} + \phi_3^{n-1} + \Delta\Gamma_{n-1}\phi_2^{n-1})]. \end{aligned} \tag{6}$$

The subscript (and superscript) n or $n-1$ denotes solution at time step n or $n-1$. The first-order explicit backward difference scheme has been adopted for the approximation of the time derivative of the velocity potential. Second-order terms in velocities, except the mean flow, have been neglected as in Reference 16. The lift and moment resultants can be calculated by integrating the pressure around the aerofoil as in Reference 16.

3. FINITE ELEMENT FORMULATION FOR SINUSOIDAL GUST

Unlike the uniform gust problem, the superposition of a sinusoidal gust on a mean flow results in a rotational flow in the whole field, which means that the governing equation is no longer the familiar Laplace equation. However, owing to the special characteristic of this rotational flow field, i.e. the curl of the velocity is only a function of x,

$$-\partial u/\partial y + \partial v/\partial x = -W_{g0}\omega \cos[\omega(x/U_\infty - t)], \tag{7}$$

so we can replace the continuous rotational flow field by a number of vertical discrete vortex lines of a 'consistent' strength. These lines are positioned at the boundary of two adjacent vertical columns of elements. This is because, in the finite element context, the only perceivable way of simulating a vortex sheet in an irrotational flow field is by applying a velocity potential difference between two layers or columns of elements. Here 'consistent' means that the vertical velocity difference between two points at some distance apart in the x-direction is the same in both the discrete and the continuous vortex system. The convenient distance for the present finite element formulation is defined as half the sum of the side lengths of the two streamwise neighbouring elements. There are, however, other choices available (see Figure 5), but Figure 5(a) is certainly the best of the three. As for fixed time step sizes, Figure 5(a) reproduces the original gust function W most closely, while Figures 5(b) and 5(c) under- or over-approximate the gust profile W respectively. To put this in another way, we use a series of step changes to approximate the original smooth gust intensity profile. As we can see, between these vortex lines we have a constant gust velocity distribution and there is a jump in gust velocity at the element boundaries. Thus the flow is irrotational in each column of elements and rotational at their boundaries. It can also be said that the initial rotational flow field is replaced by vertical finite irrotational strips divided by concentrated vortex lines, the strengths of which depend on the difference in velocities on the left and right of the vortex lines. Obviously, the more element columns we have, the better is the approximation to the gust field.

After the above simplification the governing equations and boundary condition are

$$\begin{aligned}
\nabla^2\phi &= 0 && \text{in } \Omega,\\
\partial\phi/\partial n &= u_\infty && \text{on } \partial\Omega_1,\\
\partial\phi/\partial n &= W_{g0}\sin[\omega(x/U_\infty - t)] && \text{on } \partial\Omega_2,\\
\partial n/\partial n &= 0 && \text{on } \partial\Omega_3,\\
\partial\phi &= f_1 && \text{on } \partial\Omega_4,\\
\Delta\phi &= f_2 && \text{on } \partial\Omega_5,
\end{aligned} \tag{8}$$

where f_1 and f_2 are known functions which will be explained in more detail later and $\partial\Omega_5$ is the boundary formed by the discrete vortex lines.

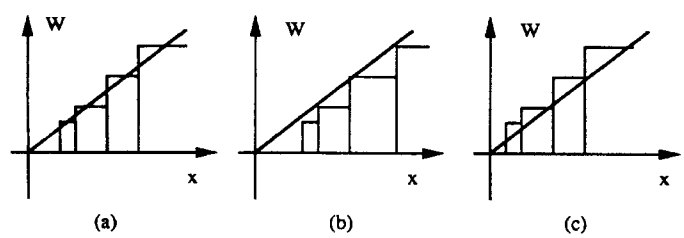

Figure 5. Different approximation schemes for sinusoidal gust

Like the problem of the oscillating aerofoil,[10] we are again treating the sinusoidal gust as a steady state problem in the frequency domain (Figure 6). The initial transient due to the aerofoil entering the gust field is not considered, since this can be dealt with by the method developed in the previous section. In contrast, the aerofoil is thought to have been in the gust for so long that a steady state has been reached. The alternating gust changes the upwash on the aerofoil periodically, which results in a corresponding change in the effective incidence. This leads to a constant flow adjustment at the trailing edge in order to satisfy the Kutta condition and the vortex shedding, which in turn produces an oscillation of the pressure on the aerofoil.

Under the small-disturbance assumption and since the mechanism of vortex shedding and wake development for the present problem is similar to that for the oscillating aerofoil, the same assumption can be made about the wake and the circulation on the aerofoil.

1. The circulation $\Gamma = \Gamma_0 + \Gamma_1 \sin(\omega t) + \Gamma_2 \cos(\omega t)$.
2. The wake is straight, infinitely thin and aligned with the freestream flow directions. Vortices are convected along it at the freestream velocity.

Hence the wake modelling for the oscillating aerofoil in Reference 10 can be used here for the sinusoidal gust. On the other hand, each of the vertical concentrated vortex lines is in fact a gust front as analysed in the previous section. Thus they can be simulated in the same manner. The only difference is that instead of one vortex line travelling downstream element-by-element, we have stationary vortex lines between every two neighbouring columns of elements.

To solve the above problem, ϕ is resolved into

$$\phi = (\phi_4 + \Gamma_0\phi_3) + (\phi_7 + \phi_6 + \Gamma_1\phi_1 + \Gamma_2\phi_2)\sin(\omega t) + (\phi_8 + \phi_5 - \Gamma_1\phi_1 + \Gamma_2\phi_2)\cos(\omega t), \quad (9)$$

where $\nabla^2\phi_i = 0$ in Ω, $\partial\phi_i/\partial n = 0$ on $\partial\Omega_3$ $(i = 1, 2, \ldots, 8)$ and

	$\partial\phi/\partial n$ on $\partial\Omega_1$	$\partial\phi$ on $\partial\Omega_2$	$\Delta\phi$ on $\partial\Omega_4$	$\Delta\phi$ on $\partial\Omega_5$
ϕ_1	0	0	$\sin(\omega s)$	0
ϕ_2	0	0	$\cos(\omega s)$	0
ϕ_3	0	0	1	0
ϕ_4	U_∞	0	0	0
ϕ_5	0	$-W_{g0}\cos(\omega x/U_\infty)\sin(\omega t)$	0	0
ϕ_6		$W_{g0}\sin(\omega x/U_\infty)\cos(\omega t)$	0	0
ϕ_7	0	0	$\Delta\phi_1$	0
ϕ_8	0	0	$\Delta\phi_2$	0

The same assumptions as in Reference 10 have been made for the circulation around the aerofoil and the wake. Hence, following the same line of thought, we can find the velocity potential difference (f_1 in equation (8)) in the wake and separate it into three parts: time- independent, ϕ_3, in-phase, ϕ_2,

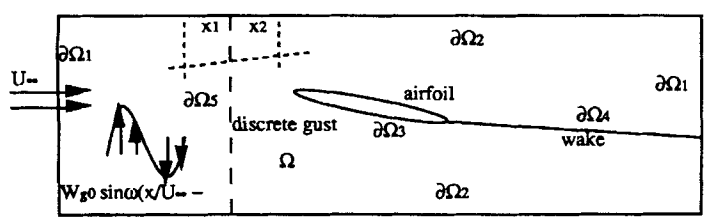

Figure 6. Problem definition of sinusoidal gust

and out-of-phase, ϕ_2, components.[10] The component ϕ_4 represents the mean flow, while ϕ_5 and ϕ_6 come from the boundary condition on $\partial\Omega_2$, namely

$$W_{g0}\sin[\omega(x/U_\infty - t)] = W_{g0}[\sin(\omega x/U_\infty)\cos(\omega t) - \cos(\omega x/U_\infty)\sin(\omega t)]. \tag{10}$$

The last two components ϕ_7 and ϕ_8 are there to simulate the discrete vortex lines. The prescribed functions f_1 and f_2 in equation (9) are

$$\Delta\phi_1 = -w_{g0}[\cos(\omega x_2/U_\infty) - \cos(\omega x_1/U_\infty)]y, \qquad \Delta\phi_2 = w_{g0}[\sin(\omega x_2/U_\infty) - \sin(\omega x_1/U_\infty)]y. \tag{11}$$

This is because the gust velocity difference between x_2 and x_1 is

$$\begin{aligned} &W_{g0}\sin[\omega(x_2/U_\infty - t)] - W_{g0}\sin[\omega(x_1/U_\infty - t)] \\ &= -[\cos(\omega x_2/U_\infty) - \cos(\omega x_1/U_\infty)]\sin(\omega t) + [\sin(\omega x_2/U_\infty) - \sin(\omega x_1/U_\infty)]\cos(\omega t), \end{aligned} \tag{12}$$

where x_2 and x_1 are the x-co- ordinates of the midside nodes of two adjacent elements.

The velocities are

$$\begin{aligned} u &= (u_4 + \Gamma_0 u_3) + (u_7 + u_6 + \Gamma_1 u_2 + \Gamma_2 u_1)\sin(\omega t) + (u_8 + u_5 - \Gamma_1 u_1 + \Gamma_2 u_2)\cos(\omega t), \\ v &= (v_4 + \Gamma_0 v_3) + (v_7 + v_6 + \Gamma_1 v_2 + \Gamma_2 v_1)\sin(\omega t) + (v_8 + v_5 - \Gamma_1 v_1 + \Gamma_2 v_2)\cos(\omega t), \end{aligned} \tag{13}$$

As in Reference 10, the smooth flow condition is adopted at the trailing edge. If we apply this condition to equation (12), we now have

$$(v_4^{TE} + \Gamma_0 v_3^{TE}) + (v_7^{TE} + v_6^{TE} + \Gamma_1 v_2^{TE} + \Gamma_2 v_1^{TE})\sin(\omega t) + (v_8^{TE} + v_5^{TE} - \Gamma_1 v_1^{TE} + \Gamma_2 v_2^{TE})\cos(\omega t) = 0. \tag{14}$$

As discussed in the last section, other forms of trailing edge conditions are possible, but for the cases in which we are interested, the above condition is sufficient. To satisfy equation (14) at any time instant, we need

$$\begin{aligned} v_4^{TE} + \Gamma_0 v_3^{TE} &= 0, \\ v_7^{TE} + v_6^{TE} + \Gamma_1 v_2^{TE} + \Gamma_2 v_1^{TE} &= 0, \\ v_8^{TE} + v_5^{TE} - \Gamma_1 v_1^{TE} + \Gamma_2 v_2^{TE} &= 0, \end{aligned} \tag{15}$$

which give

$$\begin{aligned} \Gamma_0 &= -v_4^{TE}/v_3^{TE}, \\ \Gamma_1 &= -[(v_7^{TE} + v_6^{TE})2^{TE} + (v_8^{TE} + v_5^{TE})v_1^{TE}]/(v_1^{TE}v_1^{TE} + v_2^{TE}v_2^{TE}), \\ \Gamma_2 &= -[(v_7^{TE} + v_6^{TE})v_1^{TE} + (v_8^{TE} + v_5^{TE})v_2^{TE}]/(v_1^{TE}v_1^{TE} + v_2^{TE}v_2^{TE}). \end{aligned} \tag{16}$$

The pressure can be determined by Bernoulli's theorem as

$$\begin{aligned} p &= -\rho[\partial\phi/\partial t + (u^2 + v^2)/2] \\ &= -(\rho/2)[(u_4 + \Gamma_0 u_3)^2 + (v_4 + \Gamma_0 v_3)^2] \\ &\quad (\rho/2)[(u_4 + \Gamma_0 u_3)(u_7 + u_6 + \Gamma_1 u_2 + \Gamma_2 u_1) + (v_4 + \Gamma_0 v_3)(v_7 + v_6 + \Gamma_1 v_2 + \Gamma_2 v_1) \\ &\quad - \omega(\phi_8 + \phi_5 - \Gamma_1\phi_1 + \Gamma_2\phi_2)]\sin(\omega t) \\ &\quad (\rho/2)[(u_4 + \Gamma_0 u_3)(u_8 + u_5 - \Gamma_1 u_1 + \Gamma_2 u_2) + (v_4 + \Gamma_0 v_3)(v_8 + v_5 - \Gamma_1 v_1 + \Gamma_2 v_2) \\ &\quad + \omega(\phi_7 + \phi_6 + \Gamma_1\phi_2 + \Gamma_2\phi_1)]\cos(\omega t) \\ &= p_0 + p_s\sin(\omega t) + p_c\cos(\omega t). \end{aligned} \tag{17}$$

Lift and moment resultants can be calculated as in Reference 10.

4. NUMERICAL EXAMPLES AND DISCUSSION

Stationary Gust

To validate the above theory, a calculation has been performed on a stationary gust passing a plate and an 8·4 per cent thick von Mises aerofoil. The results are shown in Figure 7 and 8. The present method provides an accurate prediction of the time history of the non-dimensionalized lift on a plate, particularly when the time increment is small and the finite element mesh is large. Figure 7 clearly demonstrates that the discrepancies at large time values are caused by numerical blockage effects. In other words, because we are using a finite mesh for an infinite problem, special treatments[17] such as geometric mapping,[18] combining with a boundary integral method,[19] asymptotic matching,[20] finite elements[21] and absorbing boundary conditions[22] are required to model the response at large times. However, they have not been considered here, since they are not the main interest of the paper. Figure 8 shows large differences between the finite element solution and that of Basu and Hancock,[6] which may be the result of the large time step employed in the present analysis. Basu and Hancock used very small time increments in their solution ($U_\infty \Delta t/C \approx 10^{-4}$), while in the present formulation the gust front has to travel at least one element in each time step. The different forms of the Kutta conditions used can also be the reason for the disagreement.

For both the above cases there is a sudden change in lift when the gust front passes through the trailing edge or when $U_\infty t/C \approx 1$. According to Basu and Hancock,[6] this is a consequence of neglecting the wake deformation. However, they believe that the time step size is at least another factor, since, as illustrated in Figure 7, when a finer mesh (i.e. smaller time steps) is employed, this sudden change is reduced.

Travelling gust

The finite element results for the travelling gust approaching from both the leading edge and the trailing edge of a plate are given in Figures 9–12. They are apparently different from the stationary normalized lift coefficient curve. One of the distinctive features is that the lift coefficient peaks when $|U_g| > 1$, and the higher the relative gust speed U_g, the sharper and stronger the peak is. Another interesting thing is that the sudden change in lift that happens with the stationary gust has now

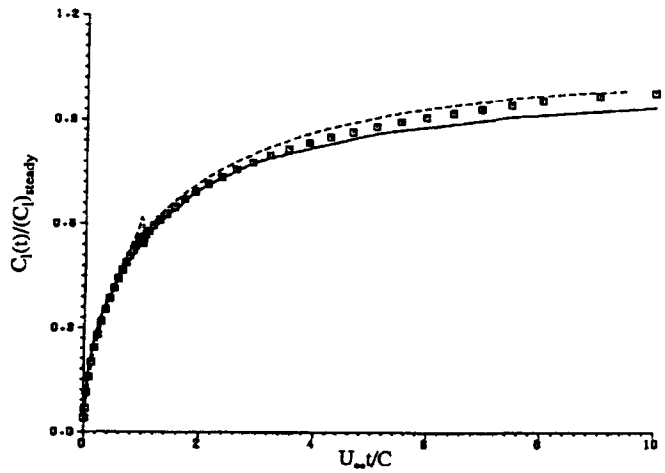

Figure 7. Plate entering a sharp-edged gust: ————, analytical; – – – –, finite element (small mesh); □, finite element (large mesh)

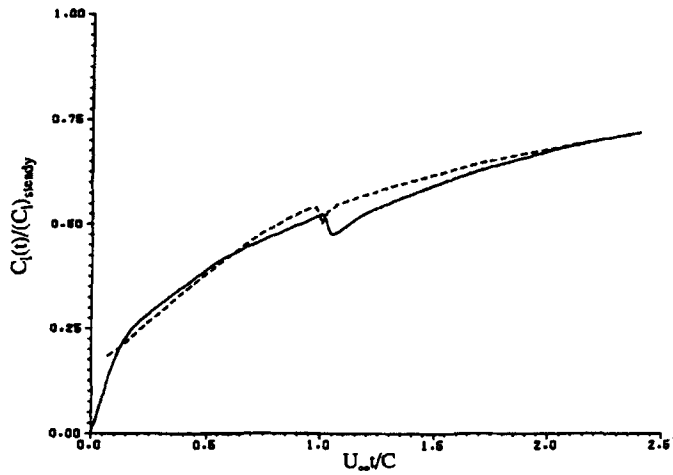

Figure 8. 8·45 thick symmetrical von Mises aerofoil entering a sharp-edged gust: ————, analytical; – – – –, finite element

disappeared. On the whole the finite element solutions are quite acceptable when the time is small, but they differ considerably from the analytical solution[7] later on. As in the previous cases, this is thought to be due to the numerical blockage effect, which seems to be more profound when the gust is travelling relative to the mean flow.

Thickness effect

The effect of aerofoil thickness on the response to a gust is again studied by comparing the time history of the non-dimensionalized lift coefficient of a symmetrical Joukowski aerofoil for thickness-to-chord ratios equal to 0 per cent, 5 per cent and 10 per cent. As can be seen in Figure 13, the thicker aerofoil has a smaller lift at the same time instant. Putting this in another way, it means that a thicker aerofoil needs a longer time to reach a steady state, which agrees with Giesing's findings.[5]

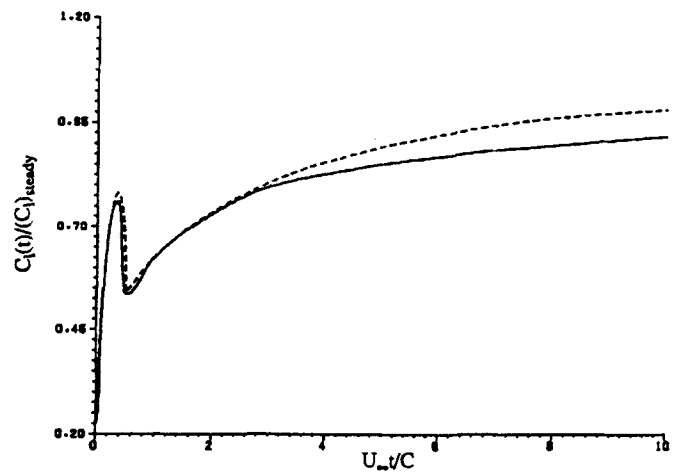

Figure 9. Travelling gust approaching from leading edge of plate, $U_g/U_\infty = 1{\cdot}0$: ————, analytical; – – – –, finite element

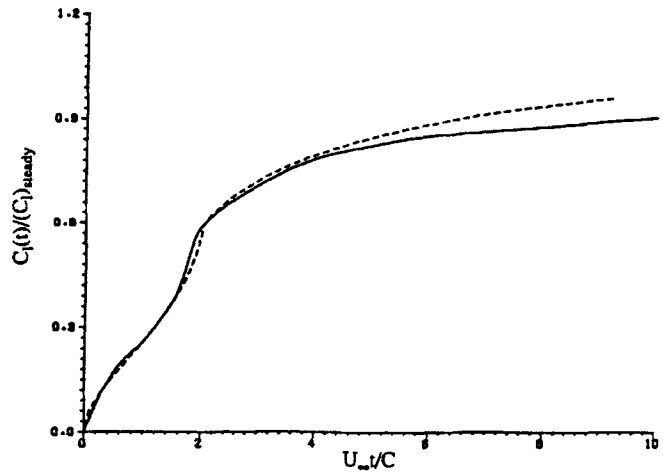

Figure 10. Travelling gust approaching from leading edge of plate, $U_g/U_\infty = -0{\cdot}5$: ————, analytical; – – – –, finite element

Sinusoidal gust

The lift coefficients of a plate and an 8·4 per cent thick symmetrical von Mises aerofoil immersed in a sinusoidal gust field are shown in Figure 14 and 15. As far as the plate is concerned, the finite element solution agrees fairly well with the exact solution, except for the out-of-phase lift coefficient at low reduced frequencies.

As before, the finite element solution shows a less satisfactory agreement with that of the panel method for the 8·4 per cent von Mises aerofoil. The reasons are believed to be the same: the mesh size and density, the form of the Kutta condition employed and the artificial reflection at boundaries.

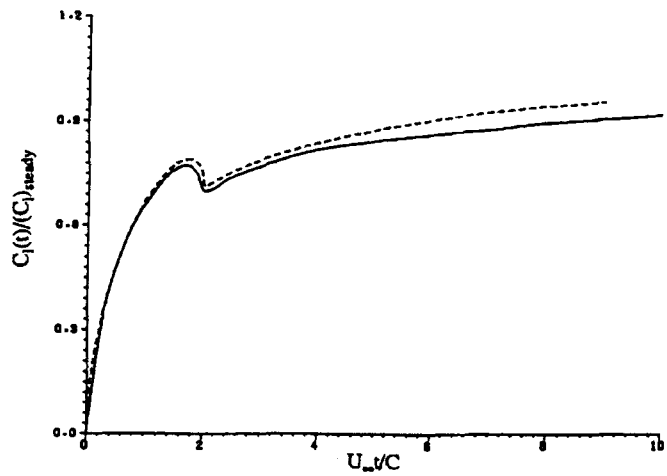

Figure 11. Travelling gust approaching from trailing edge of plate, $U_g/U_\infty = -1{\cdot}5$: ————, analytical; – – – –, finite element

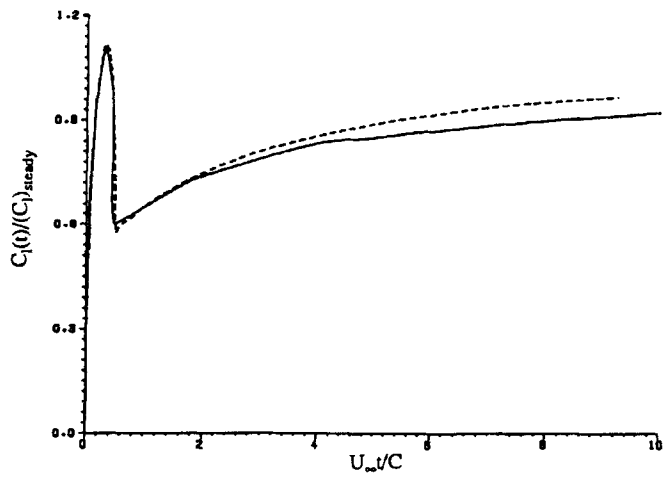

Figure 12. Travelling gust approaching from trailing edge of plate, $U_g/U_\infty = -3{\cdot}0$: ————, analytical; – – – –, finite element

5. CONCLUSIONS

In this paper a finite element formulation for both the stationary and the travelling uniform sharp-edged gust has been developed and tested for a number of cases for which analytical solutions are available. The effect of thickness on the gust loading has also been studied. A large part of the simulation (especially for the wake) has been borrowed directly from our previous papers.[10,16,17] The novel phenomenon for the present gust problem is the existence of a moving gust front. Because it has been idealized as a vortex sheet, the gust front can also be modelled by a distribution of velocity potential difference as has been done for the wake. Since a gust of arbitrary profile can be approximated by the sum of uniform sharp-edged gusts, the present formulation can handle a gust of arbitrary intensity. This can be realized by placing an appropriate number of vortex lines or gust

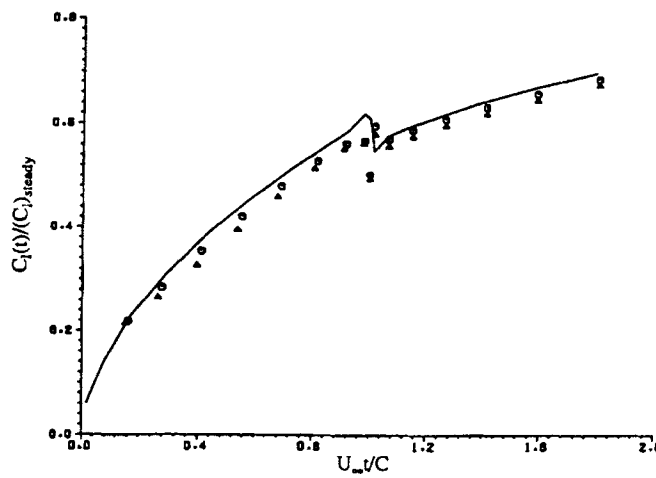

Figure 13. Thickness effect on Kussner function: ————, plate; ○, 5% thick; ▲, 10% thick

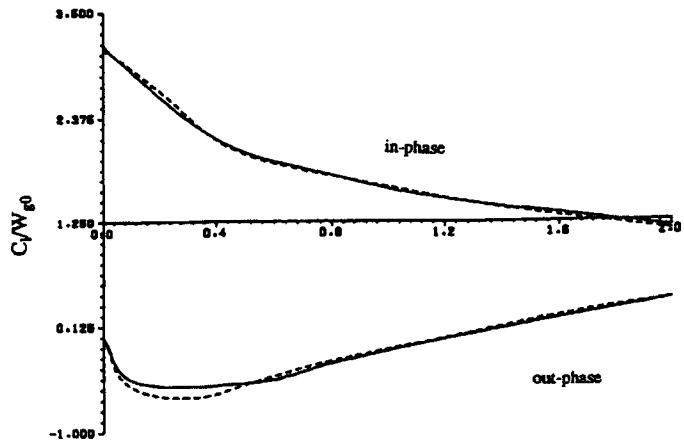

Figure 14. Response of plate to sinusoidal gust: ————, analytical; – – – –, finite element

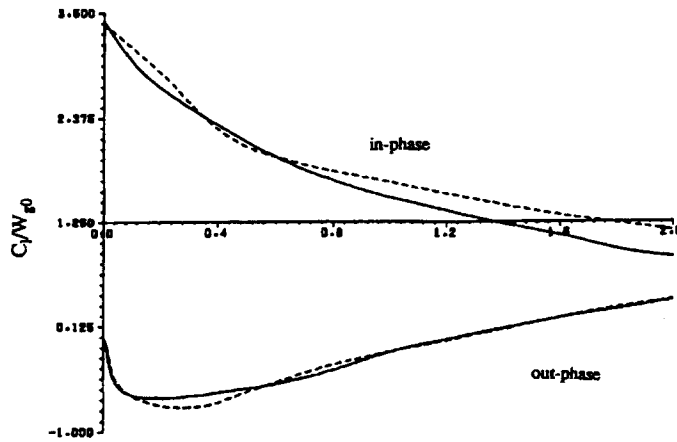

Figure 15. Response of 8·4 per cent thick symmetrical von Mises aerofoil to sinusoidal gust: ————, analytical; – – – –, finite element

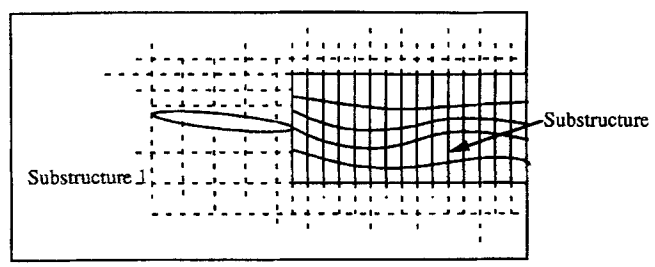

Figure 16. Substructure model for large wake deformation

fronts in the flow field instead of just one gust front. These gust fronts have to travel the same distance within each time step.

To simplify the problem, a number of assumptions have been made to achieve a linearized problem. For example, the wake (and the gust front) was assumed to be straight. However, this assumption can be removed and those elements close to the wake can be allowed to deform with it, which suggests that the solution must be carried out in the time domain and the element matrices have to be reformed at each time step. Since only those elements next to the wake need to have finite displacements to trace the wake distortion, they can be treated as a substructure (Figure 16). The element matrix reformulation is done only in this part, while the rest of the elements make up another substructure and their matrices remain unchanged. This, nevertheless, is still unable to model a severe wake distortion such as vortex roll-up.

REFERENCES

1. 'An introduction to time-dependent aerodynamics of aircraft response, gust and active control', *ESDU 84020*, 1984.
2. H. G. Kussner, 'Zusammenfassender Bericht uber den Instationaren auftrieb von Tragflügeln', *Luftfahrrttforschung*, **13**, 410–424 (1936).
3. T. von Karman and W. R. Sears, 'Aerofoil theory for nonuniform motions', *J. Aeronaut. Sci.*, **5**, 378–390 (1938).
4. T. Theodorsen, 'General theory of aerodynamic instability and the mechanism of flutter', *NACA Rep. 496*, 1934.
5. J. P. Giesing, 'Nonlinear two-dimensional unsteady flow with lift', *J. Aircraft*, **5**, 135 (1968).
6. B. C. Basu and G. J. Hancock, 'The unsteady motion of a two- dimensional aerofoil in incompressible inviscid flow', *J. Fluid Mech.*, **87**, 159 (1978).
7. J. A. Drischler and F. W. Diederich, 'Lift and moment responses to penetration of sharp-edged travelling gusts, with application to penetration of weak blast waves', *NACA TN3956*, 1957.
8. J. W. Miles, 'The aerodynamic force on an aerofoil in a moving gust– -a generalization of the 2D gust problem', *Rep. SM-18598*, Douglas Aircraft Co., 1954.
9. J. A. Drischler, 'Calculation and compilation of the unsteady lift functions for rigid wings subjected to sinusoidal gusts and to sinusoidal sinking oscillations', *NACA TN3748*, 1956.
10. J. Shi and D. Hitchings, 'Calculation of flutter derivatives and speed by finite element method', *Appl. Math. Model.*, **18**, 538- -549 (1994).
11. J. P. Giesing, W. P. Rodden and B. Stall, 'Sears function and lifting surface theory for harmonic gust fields', *J. Aircraft*, **7**, 252 (1970).
12. B. C. Basu and G. J. Hancock, '2D aerofoils and control surfaces in simple harmonic motion in incompressible inviscid flow', *ARC CP 1392*, 1978.
13. W. R. Sears, 'Some aspects of non-stationary aerofoil theory and its practical application', *J. Aeronaut. Sci.*, **8**, 104–108 (1941).
14. R. T. Jones, 'The unsteady lift of a wing of finite aspect ratio', *NACA Rep. 687*, 1940.
15. I. E. Garrick, 'On some reciprocal relations in the theory of non- stationary flows', *NACA Rep. 629*, 1936.
16. J. Shi and D. Hitchings, 'Indical lift build-up on aerofoils studied by the finite element method', *Int. j. numer. methods fluids*, **17**, 401–416 (1993).
17. J. Shi and D. Hitchings, 'An accurate finite element method for 2D aerofoil problems', *Int. J. Commun. Appl. Numer. Methods*, **10**, 155–166 (1994).
18. D. K. Gartling, 'Finite element analysis of viscous incompressible fluid flow', *Comput. Method Appl. Mech. Eng.*, **8**, 51–60 (1976).
19. C. A. Fellipa, 'Interfacing finite element and boundary element discretization', *Appl. Math. Model.*, **5**, 383–386 (1981).
20. W. G. Habashi, 'The finite element method in the solution of unbounded potential flows', *Int. j. numer. methods eng.*, **14**, 1347–1358 (1979).
21. P. Bettess, 'Infinite elements', *Int. j. numer. methods eng.*, **11**, 53–64 (1977).
22. B. Engquist, 'Absorbing boundary condition for the numerical solution of waves', *Math. Comput.*, **31**, 629–651 (1977).